Jaime Fabián Nieto Castellanos

September 2, 2021

High precision results

The following results were obtained through several simulations on lattices of size 6×64, 7×64, 8×64, 9×64, 10×64, 11×64 and 12×64 with the parameters shown in Table 1

Ntime	64
Ntherm	1000
Nmeasure	10000
Trajectory Steps	10
Nsteps	20
β	2

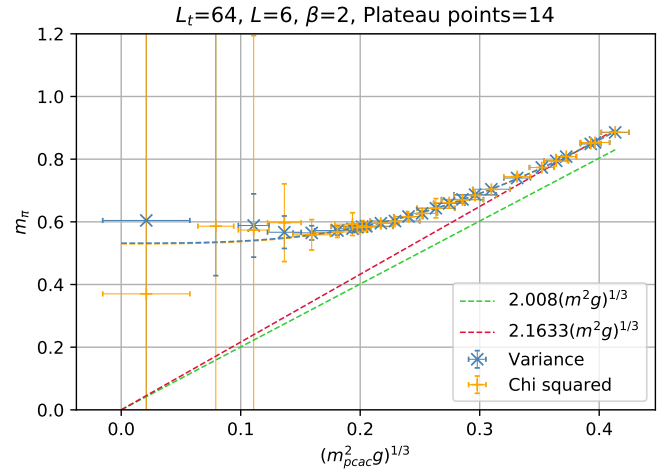Table 1: All the simulations were performed with this parameters.

Variance stands for the var option in the masscoll program and Chi squared for the χ^2 option. $g = \frac{1}{\sqrt{\beta}}$. The residual pion mass is extrapolated with two different methods. In the plots of m_π vs. $(g\, m_{pcac}^2)^{1/3}$ we fit a function of the form
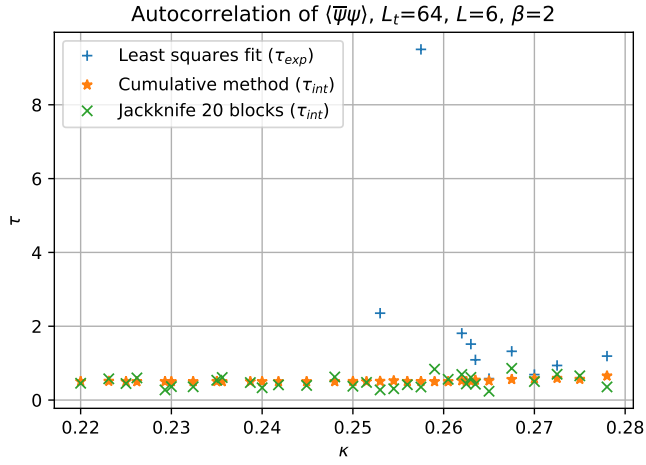
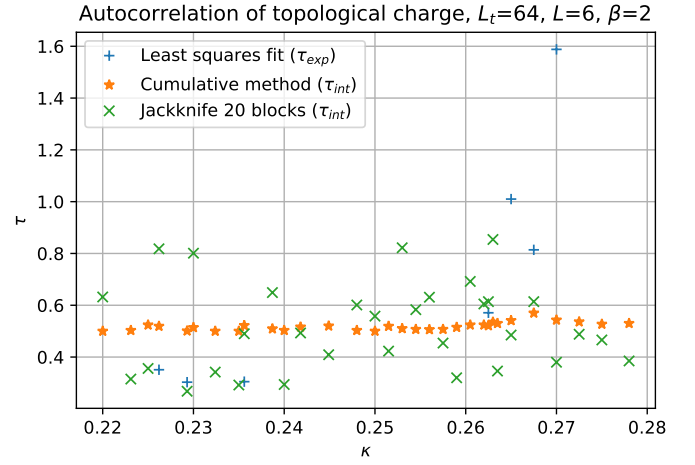$$y = \sqrt{a + bx^3}. \tag{1}$$

6x64
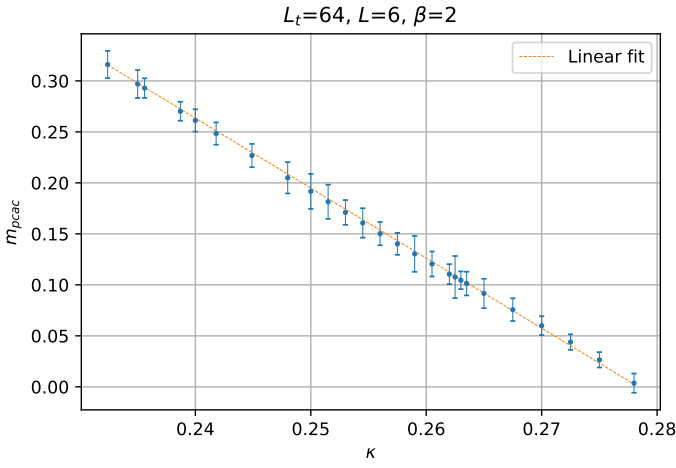
(a) Fermion mass using PCAC relation.

(b) A function of the form $y = \sqrt{a + bx^3}$ was fitted. Only $m_{pcac} > 0$ is considered.

(c) Autocorrelation of $\langle \overline{\psi}\psi \rangle$
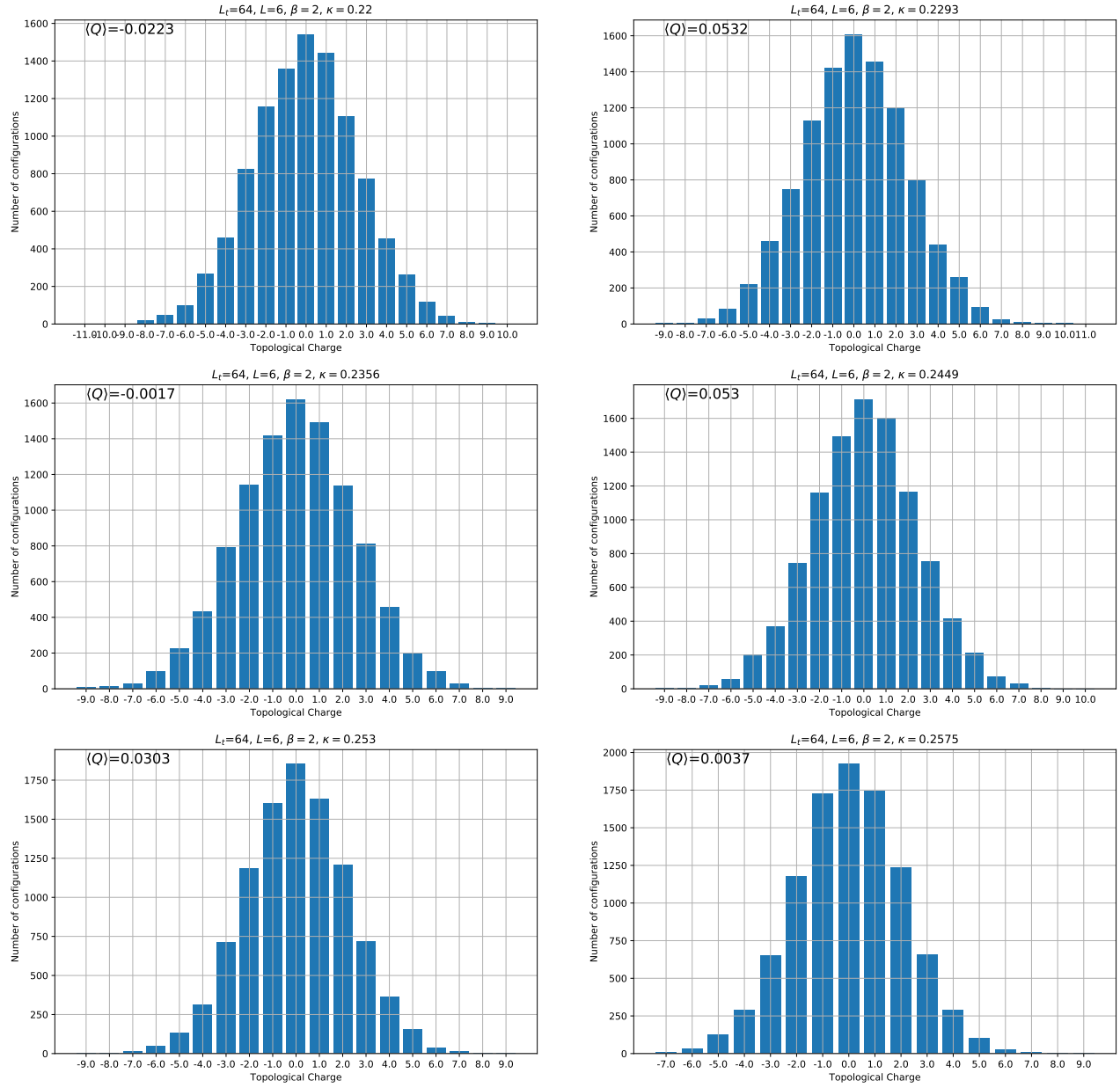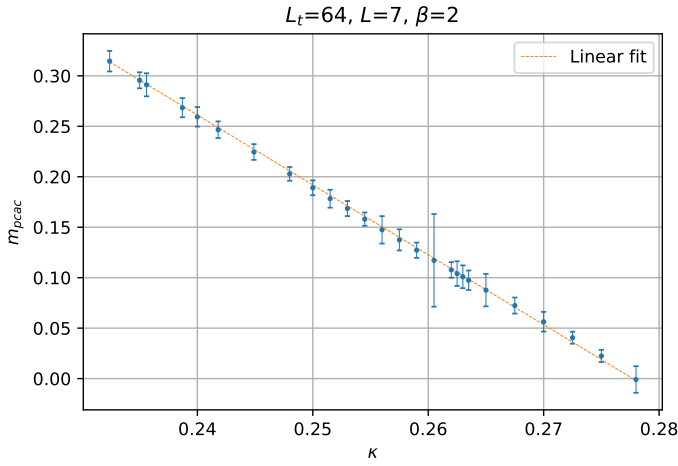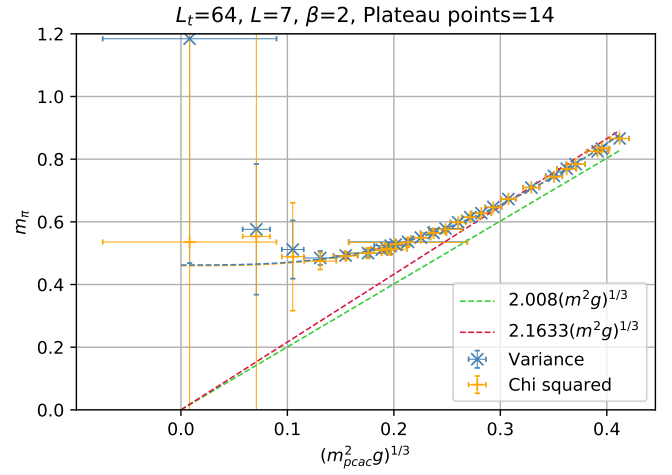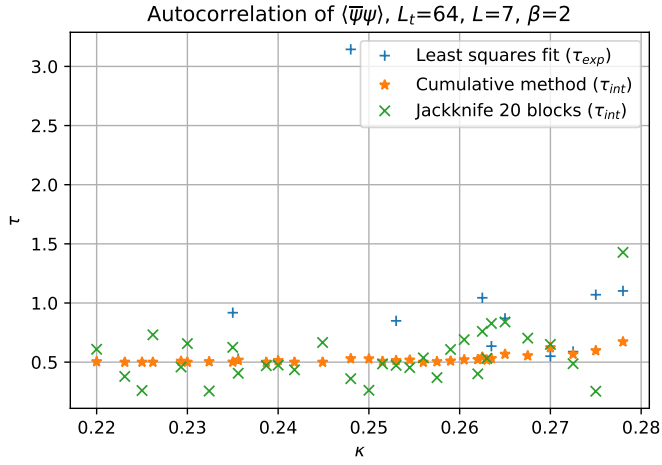
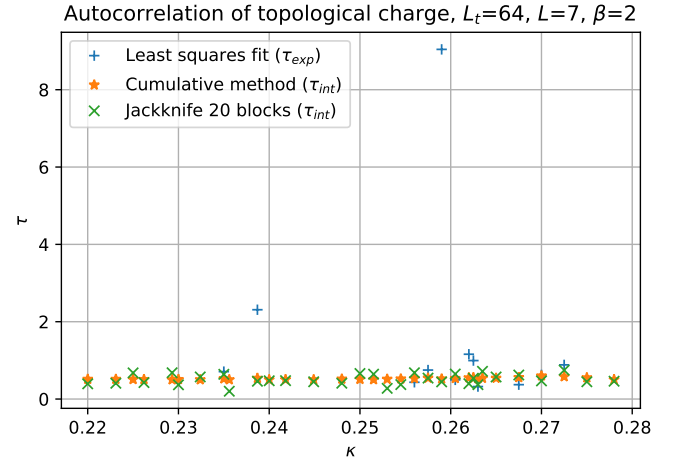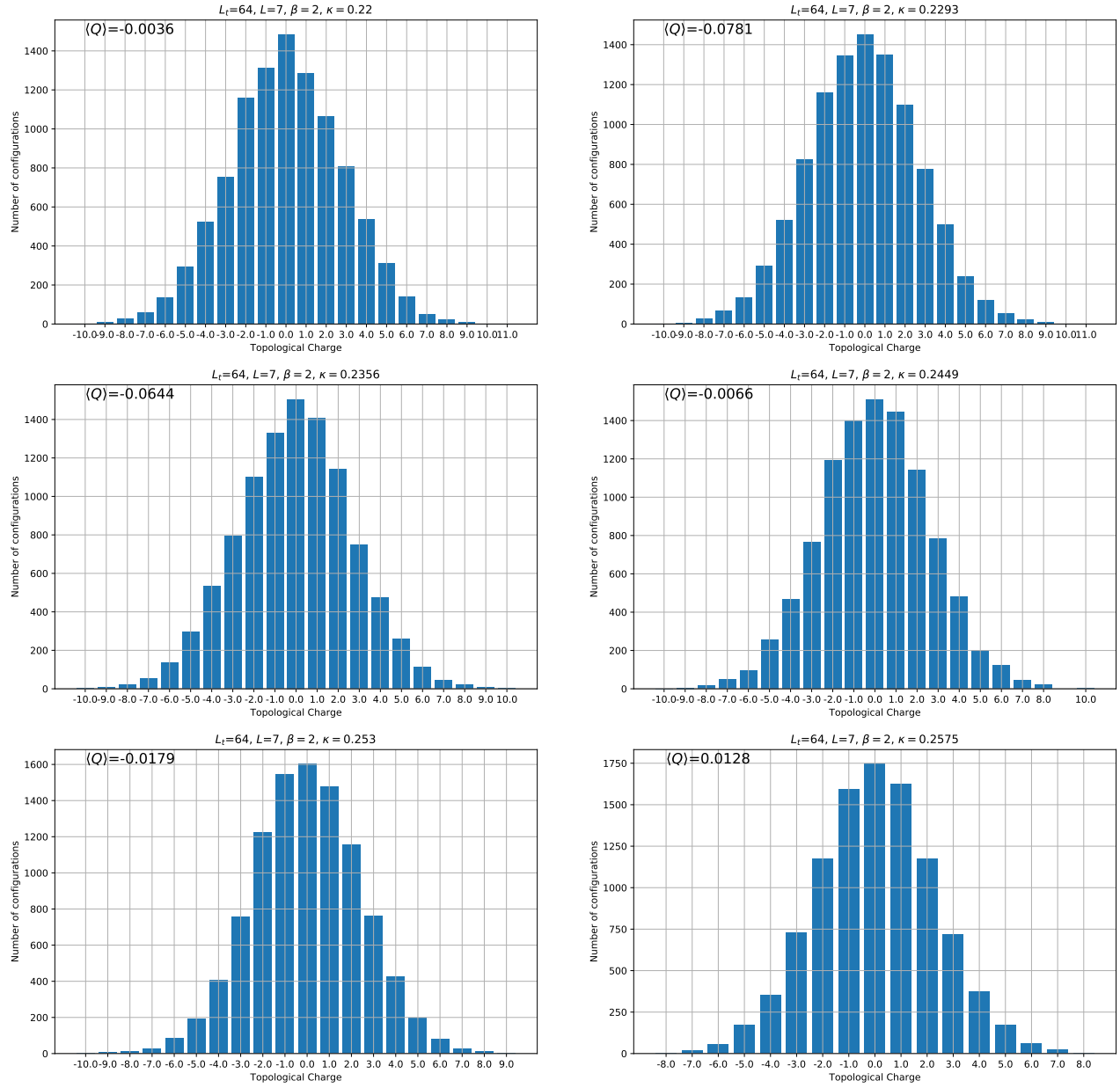(d) Autocorrelation of the topological charge

Figure 1: Number of configurations vs. topological charge on a 6×64 lattice.

7x64

(a) Fermion mass using PCAC relation.

(b) A function of the form $y = \sqrt{a + bx^3}$ was fitted. Only $m_{pcac} > 0$ is considered.

(c) Autocorrelation of $\langle \overline{\psi}\psi \rangle$
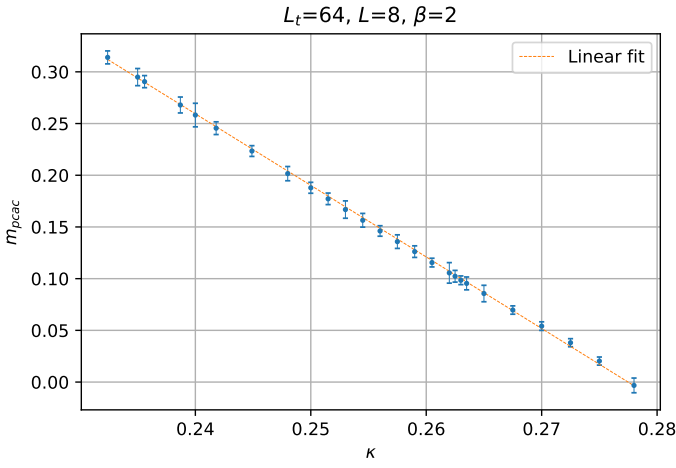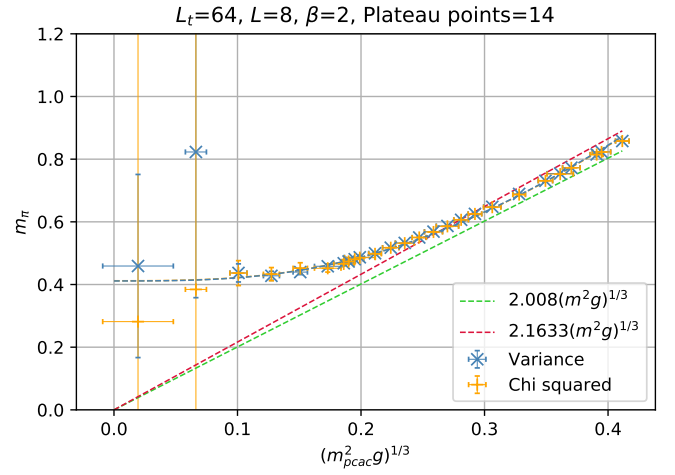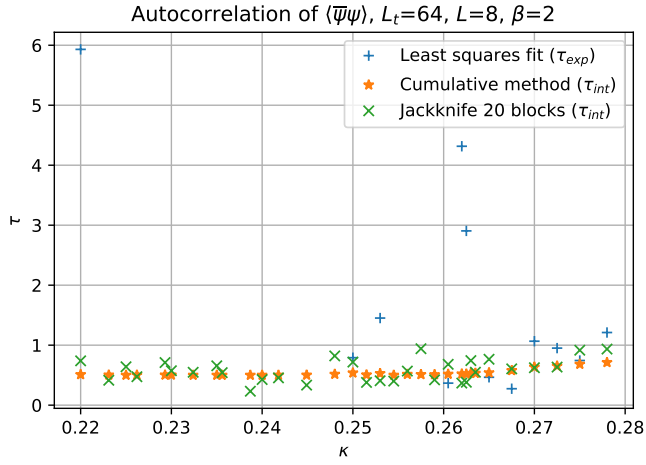
(d) Autocorrelation of the topological charge

Figure 2: Number of configurations vs. topological charge on a 7×64 lattice.
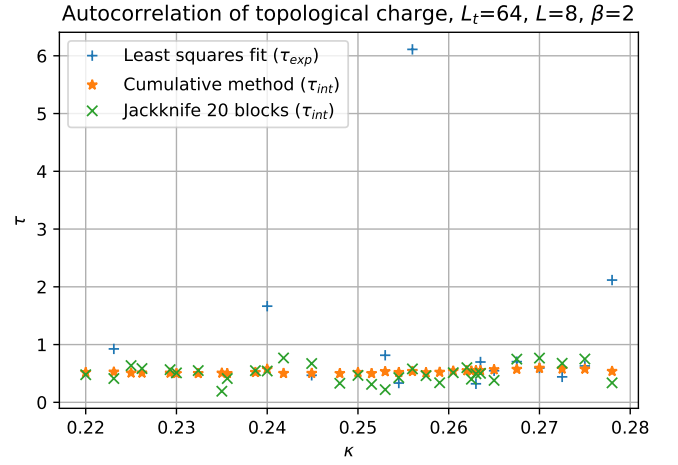
8x64

(a) Fermion mass using PCAC relation.

(b) A function of the form $y = \sqrt{a + bx^3}$ was fitted. Only $m_{pcac} > 0$ is considered.

(c) Autocorrelation of $\langle \overline{\psi}\psi \rangle$
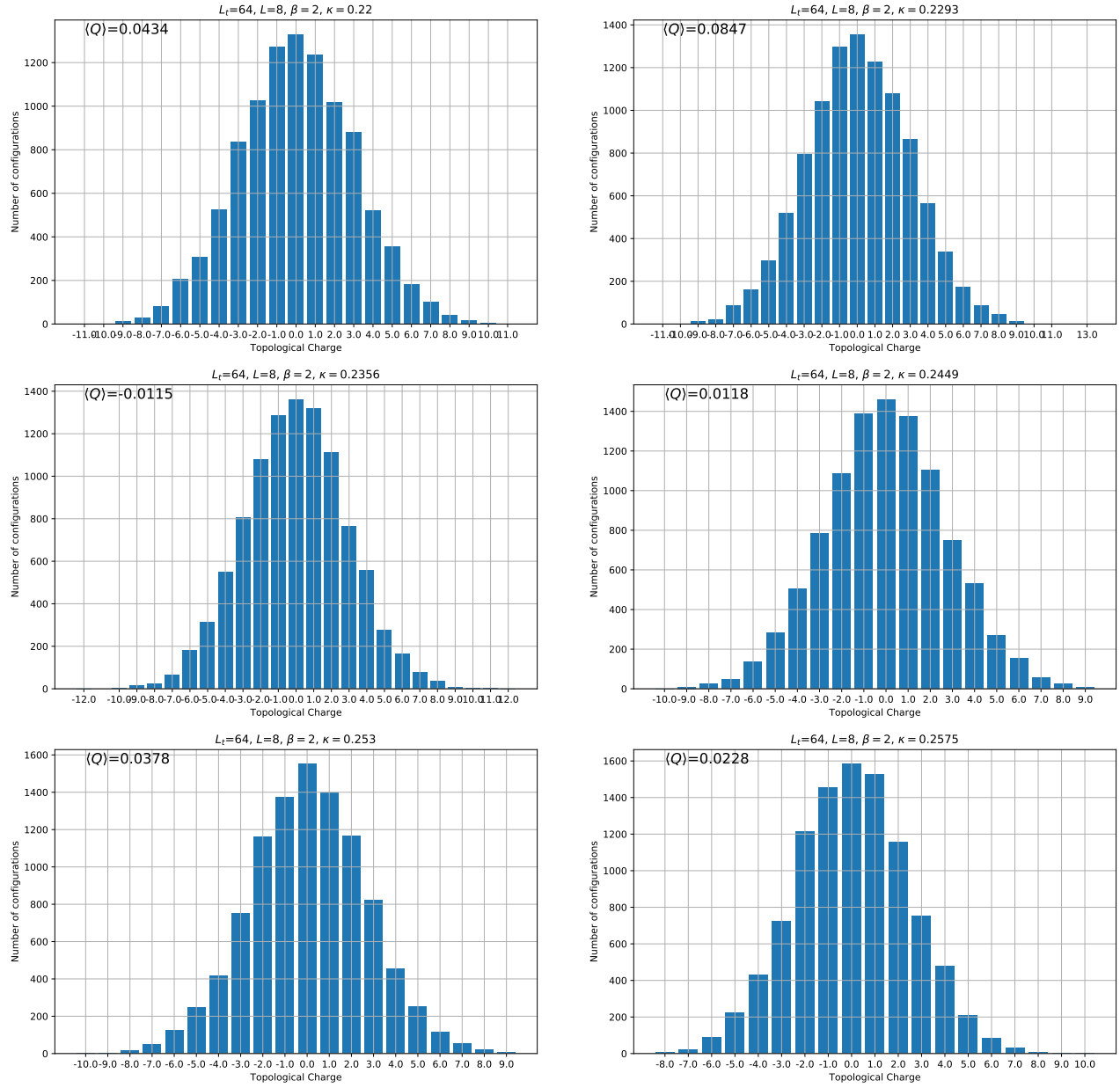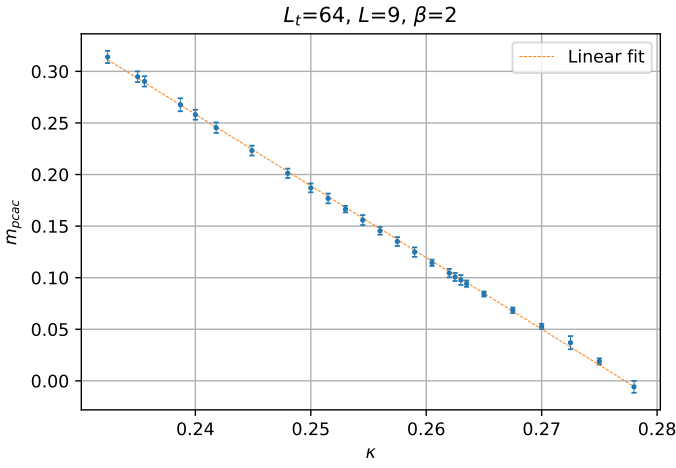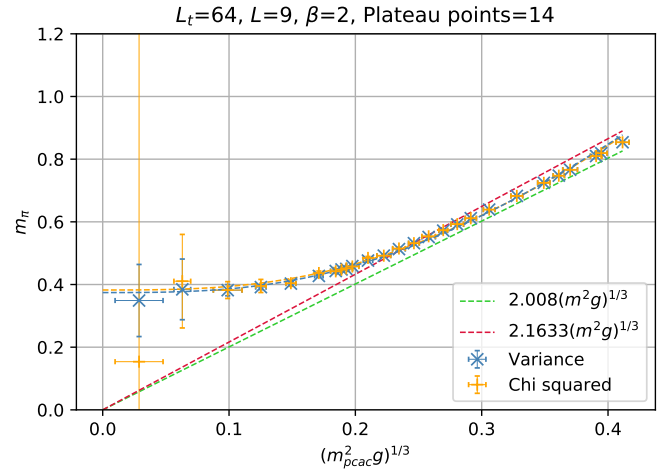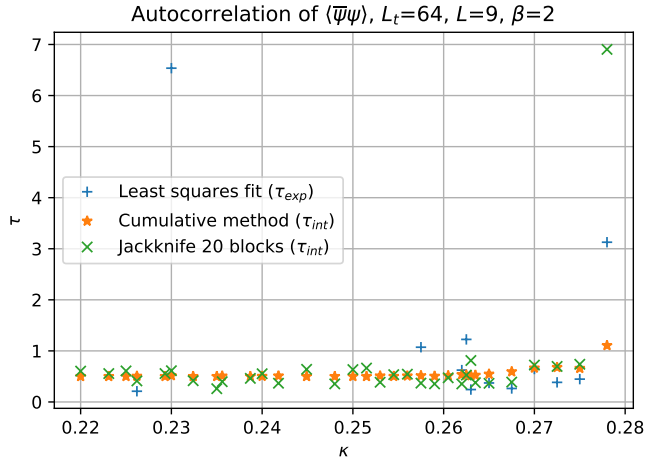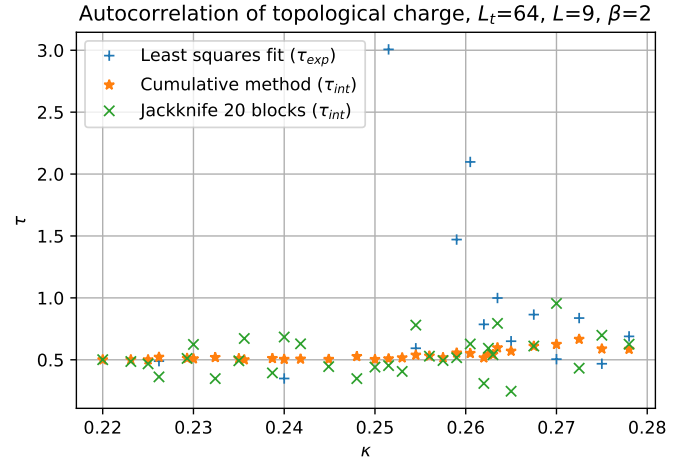
(d) Autocorrelation of the topological charge

Figure 3: Number of configurations vs. topological charge on a 8×64 lattice.

(a) Fermion mass using PCAC relation.

(b) A function of the form $y = \sqrt{a + bx^3}$ was fitted. Only $m_{pcac} > 0$ is considered.

(c) Autocorrelation of $\langle \overline{\psi}\psi \rangle$

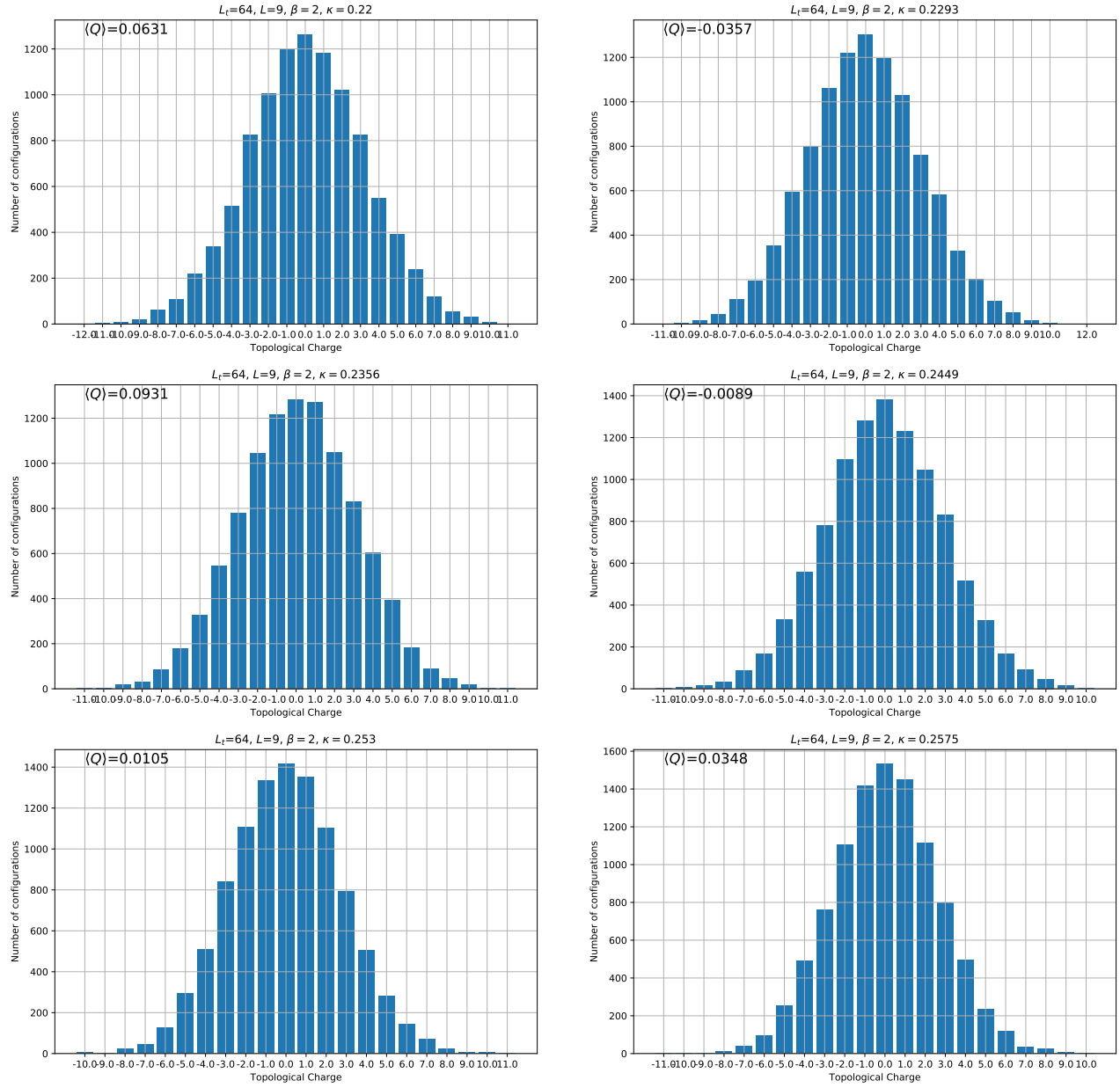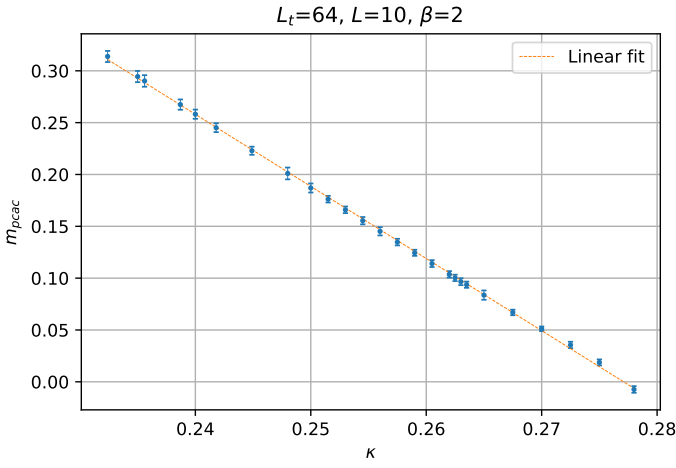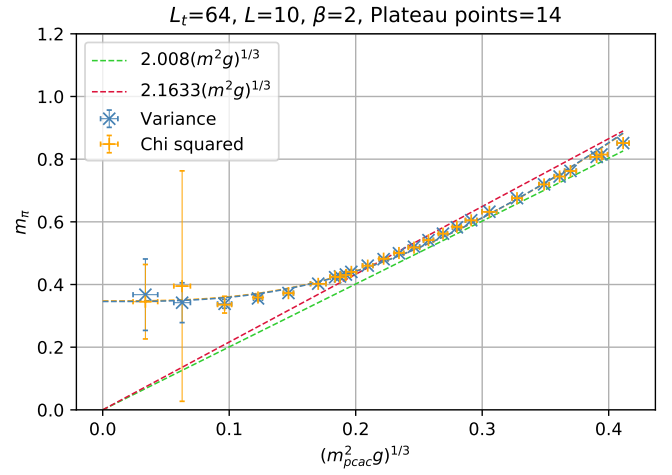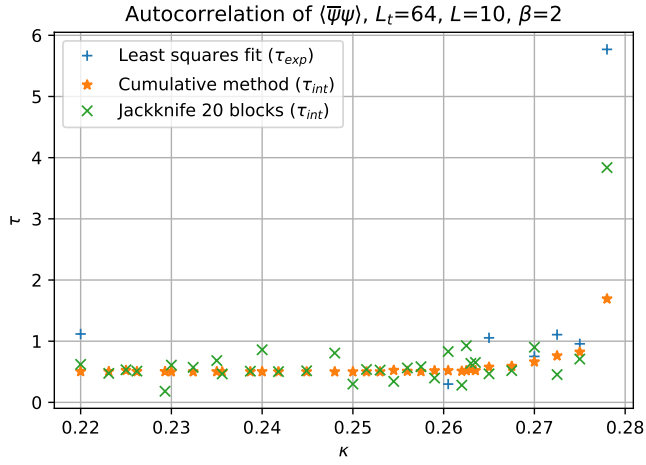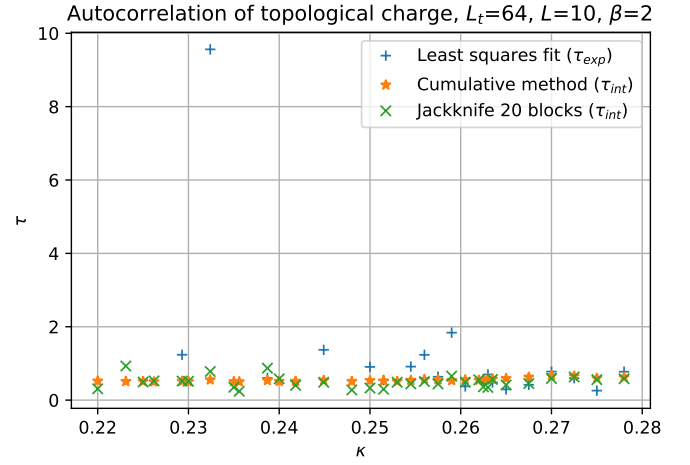(d) Autocorrelation of the topological charge

Figure 4: Number of configurations vs. topological charge on a 9×64 lattice.

(a) Fermion mass using PCAC relation.

(b) A function of the form $y = \sqrt{a + bx^3}$ was fitted. Only $m_{pcac} > 0$ is considered.

(c) Autocorrelation of $\langle \overline{\psi}\psi \rangle$

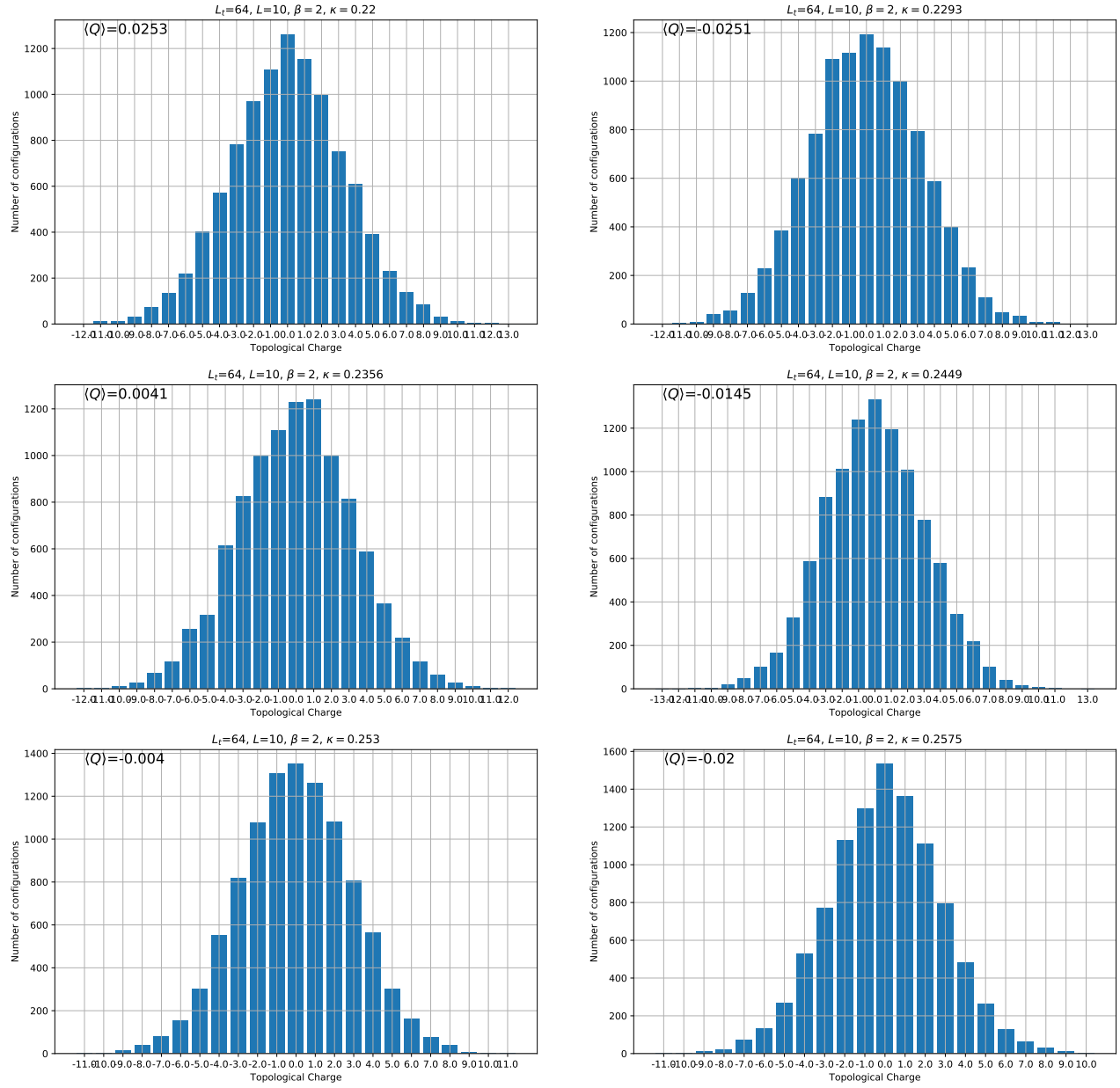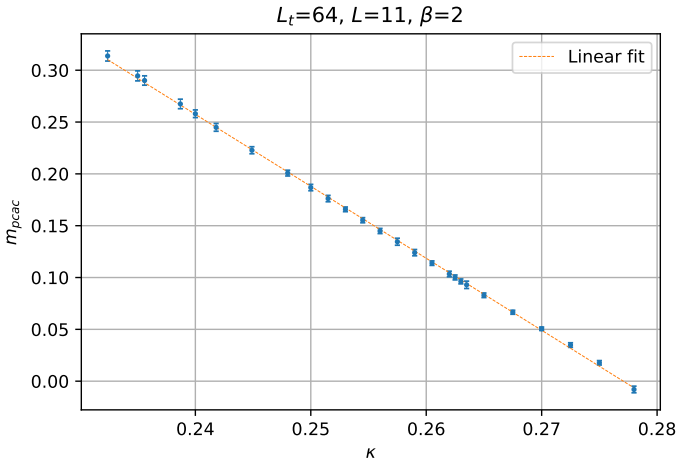(d) Autocorrelation of the topological charge

Figure 5: Number of configurations vs. topological charge on a 10×64 lattice.

11x64

(a) Fermion mass using PCAC relation.

(b) A function of the form $y = \sqrt{a + bx^3}$ was fitted. Only $m_{pcac} > 0$ is considered.

(c) Autocorrelation of $\langle \overline{\psi}\psi \rangle$
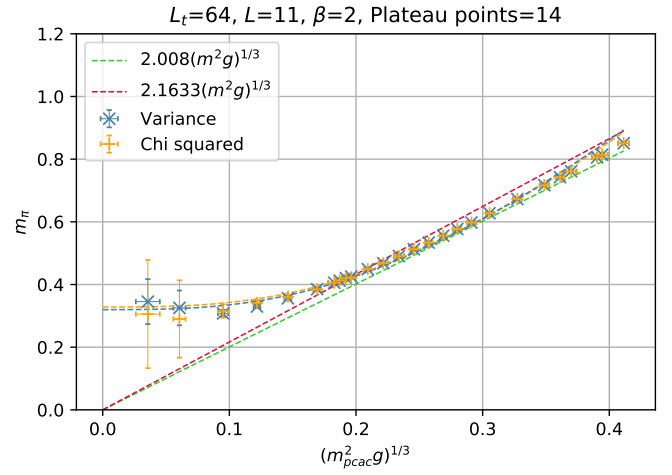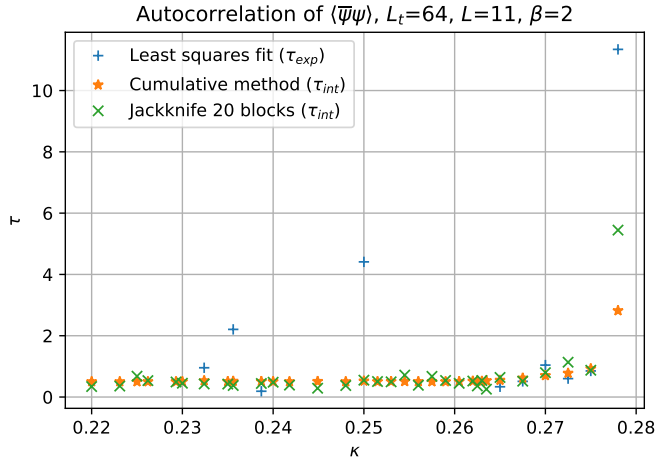
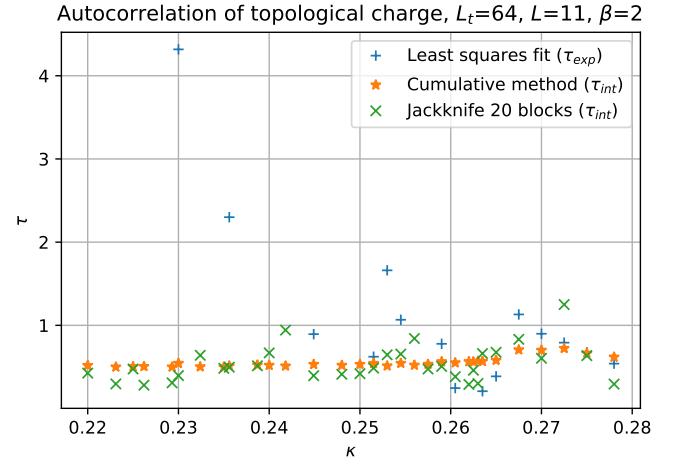(d) Autocorrelation of the topological charge

Figure 6: Number of configurations vs. topological charge on a 11×64 lattice.

12x64

(a) Fermion mass using PCAC relation.

(b) A function of the form $y = \sqrt{a + bx^3}$ was fitted. Only $m_{pcac} > 0$ is considered.

(c) Autocorrelation of $\langle \overline{\psi}\psi \rangle$

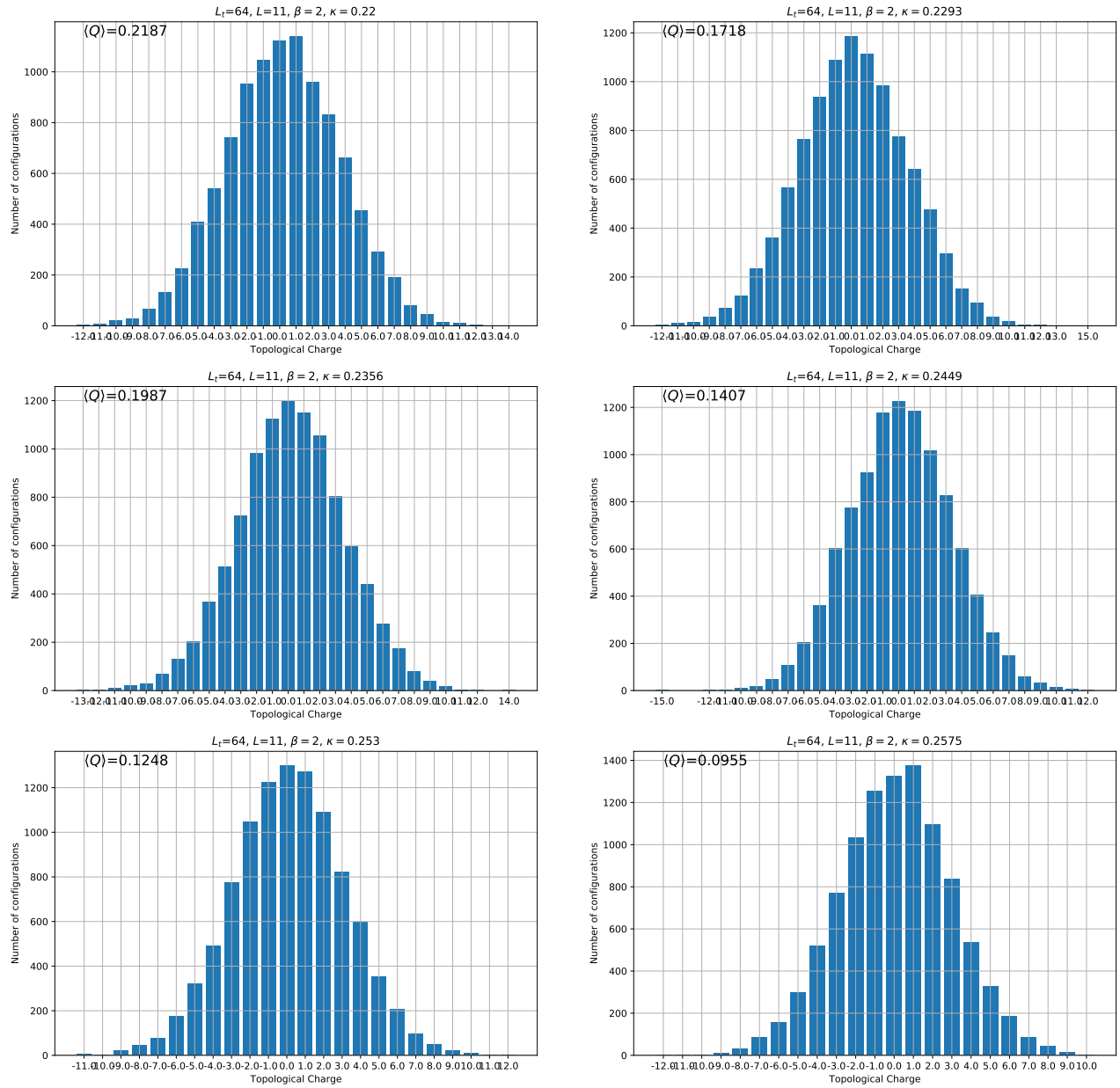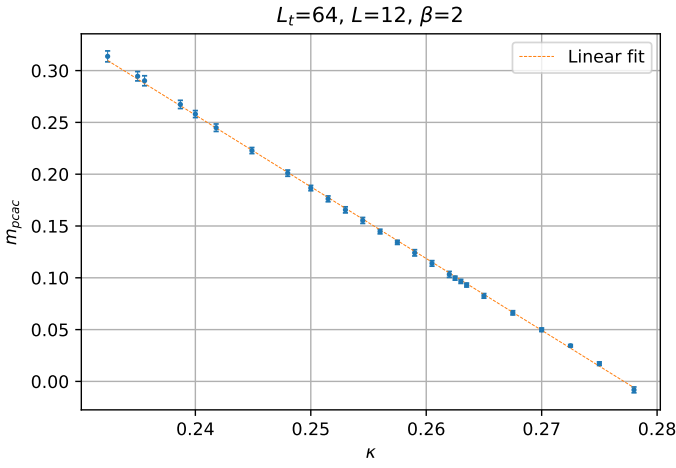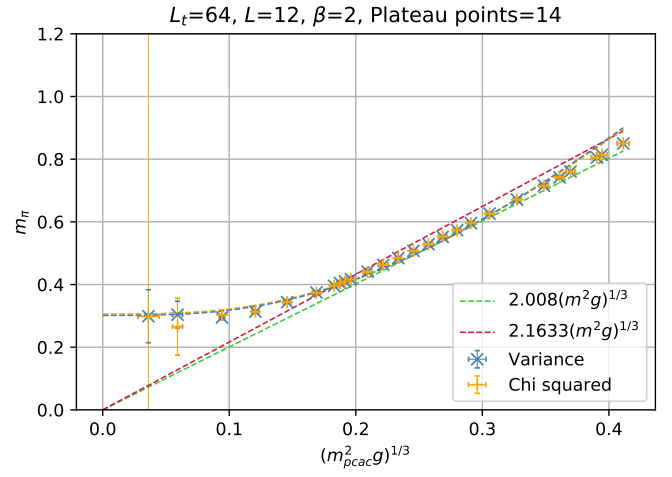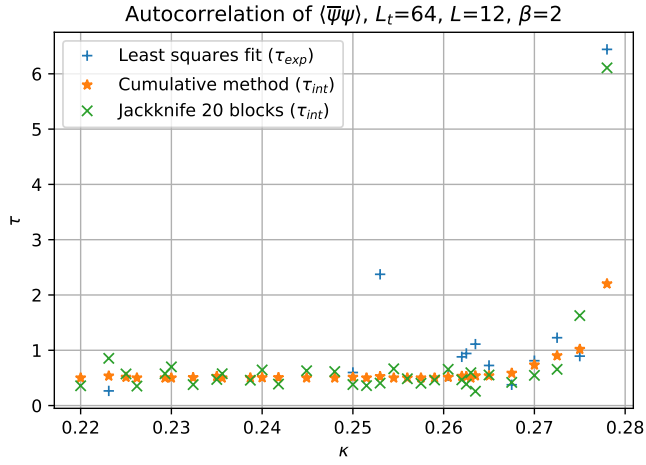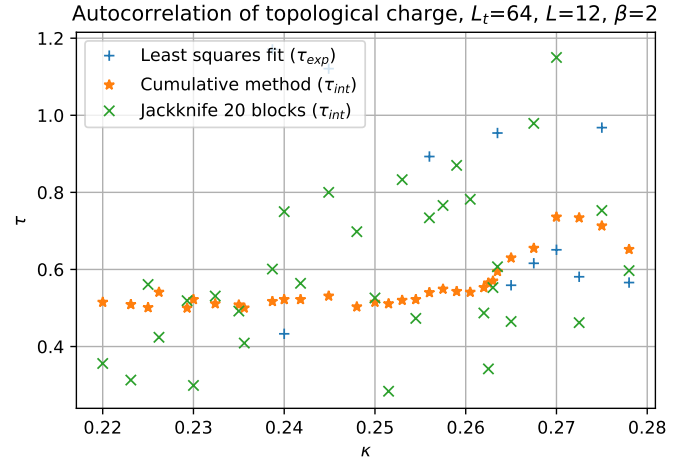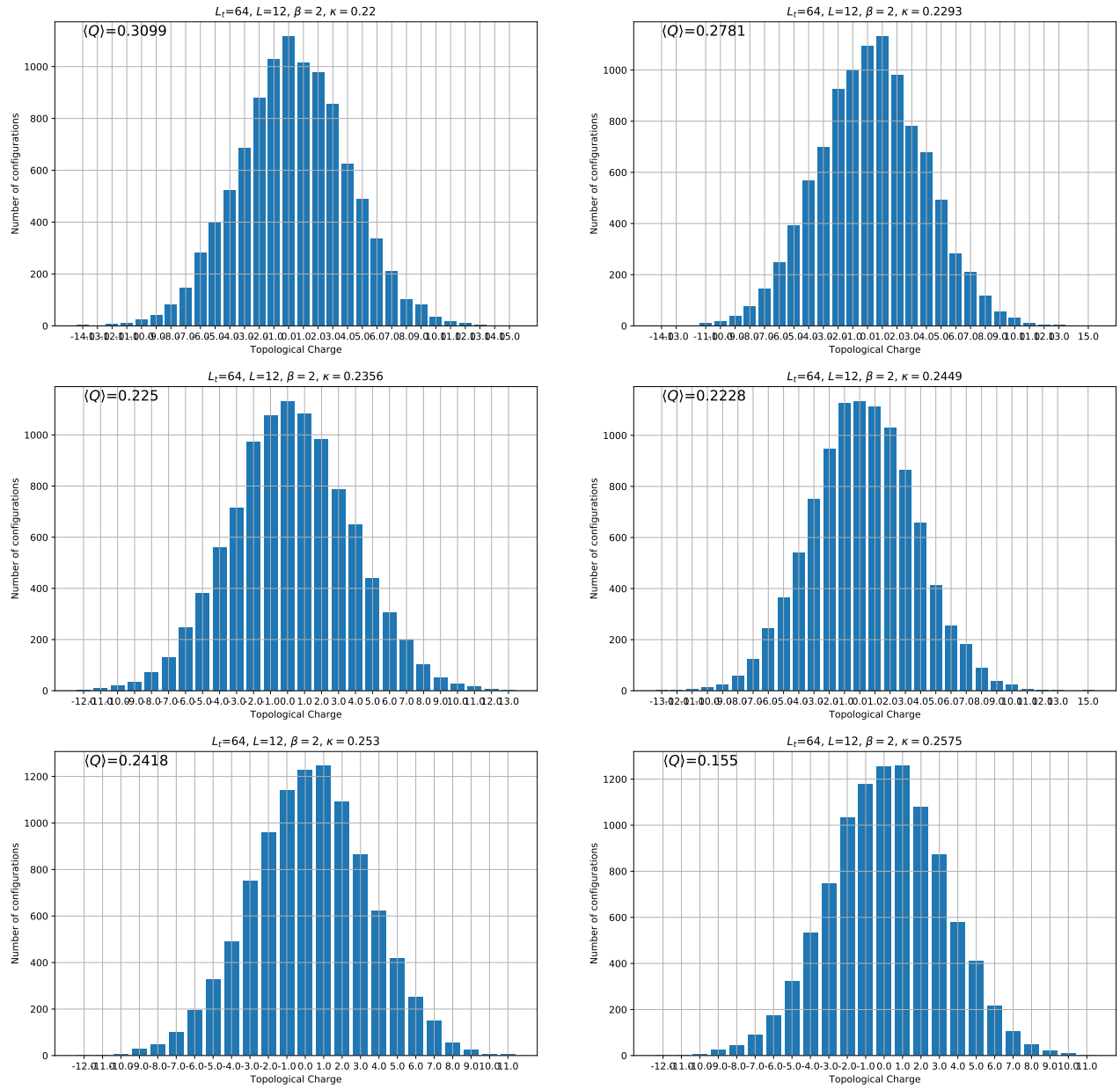(d) Autocorrelation of the topological charge

Figure 7: Number of configurations vs. topological charge on a 12×64 lattice.
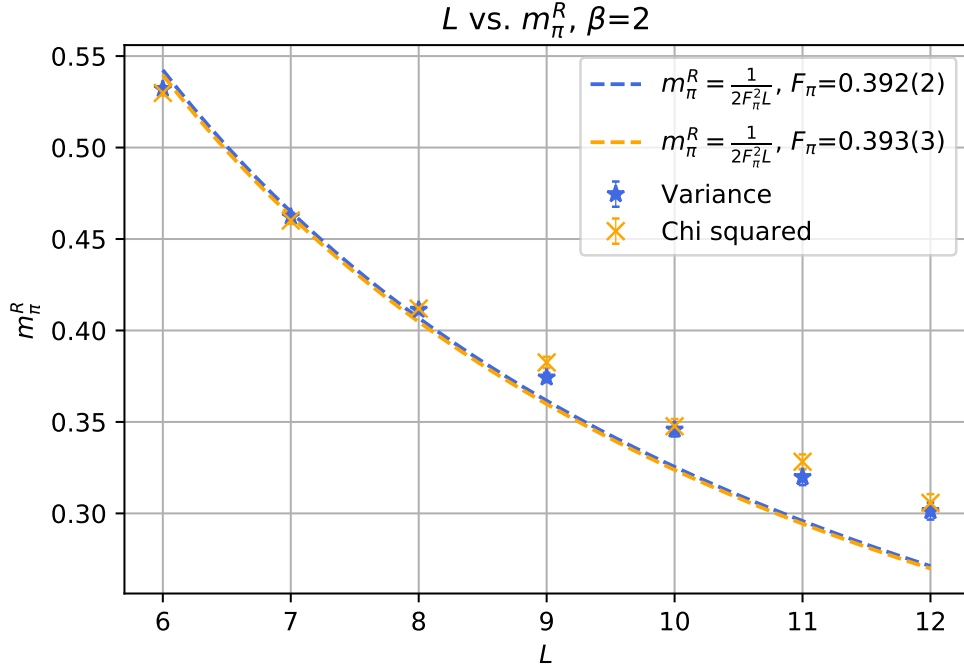
F_π extrapolation

Figure 8: m_π^R vs. L. We fitted a function of the form $y = a/x$. For variance $F_\pi = 0.392(2)$, while for chi squared $F_\pi = 0.393(3)$.
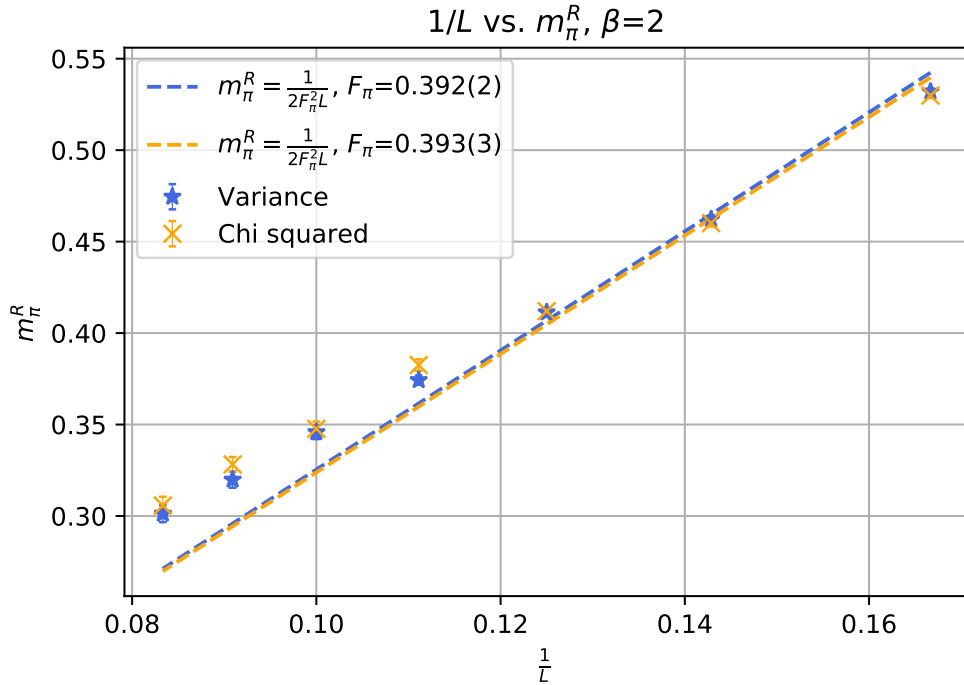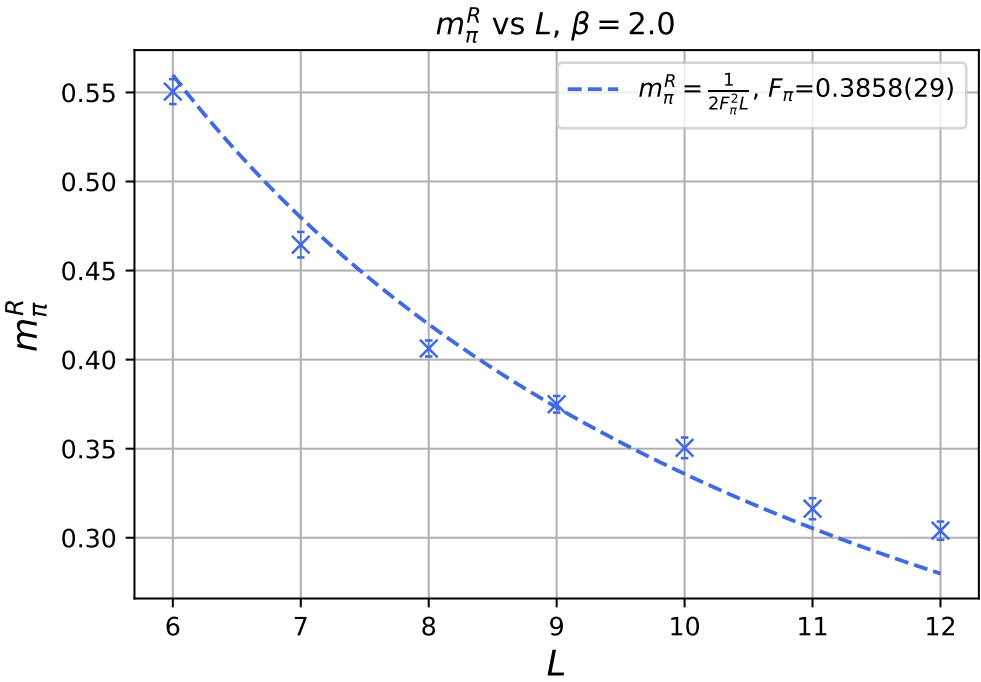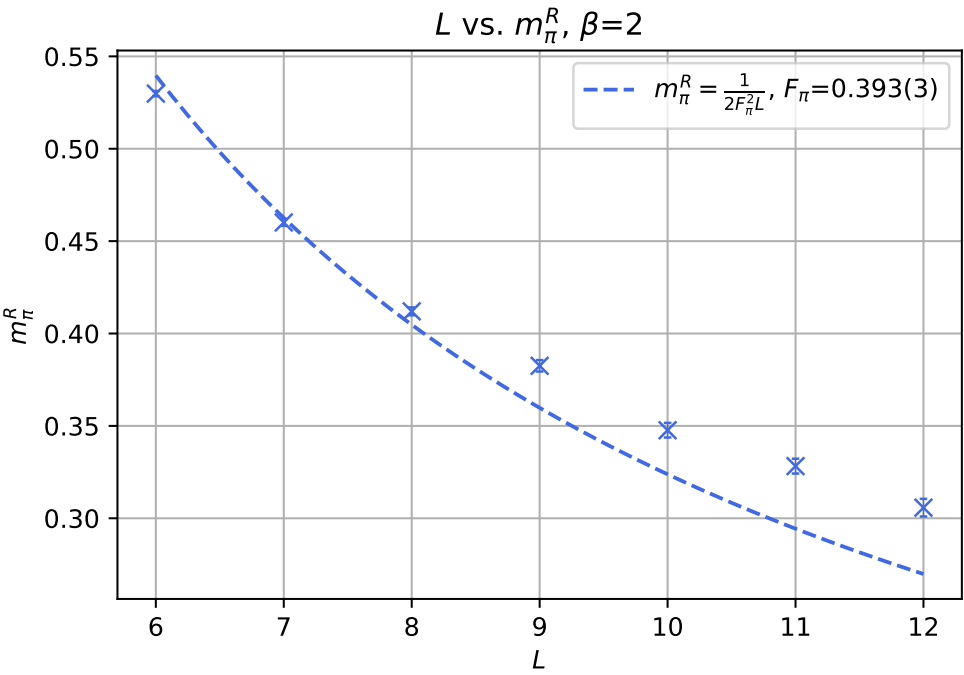

Figure 9: m_π^R vs. $1/L$. We fitted a function of the form $y = a/x$. For variance $F_\pi = 0.392(2)$, while for chi squared $F_\pi = 0.393(3)$.

Comparison with the low statistics results

(a) Results with low statistics $\backsim 10^3$ measurements.

(b) Results with high statistics $\backsim 10^4$ measurements.